

University of Texas Rio Grande Valley

ScholarWorks @ UTRGV

Physics and Astronomy Faculty Publications
and Presentations

College of Sciences

1-10-2012

Observability of pulsar beam bending by the Sgr A* black hole


Kevin Stovall

Teviet Creighton

Richard H. Price

Fredrick A. Jenet

Follow this and additional works at: https://scholarworks.utrgv.edu/pa_fac

 Part of the [Astrophysics and Astronomy Commons](#)

Recommended Citation

Kevin Stovall, et. al., (2012) Observability of pulsar beam bending by the Sgr A* black hole. *Astrophysical Journal* 744:2. DOI: <http://doi.org/10.1088/0004-637X/744/2/143>

This Article is brought to you for free and open access by the College of Sciences at ScholarWorks @ UTRGV. It has been accepted for inclusion in Physics and Astronomy Faculty Publications and Presentations by an authorized administrator of ScholarWorks @ UTRGV. For more information, please contact justin.white@utrgv.edu, william.flores01@utrgv.edu.

OBSERVABILITY OF PULSAR BEAM BENDING BY THE Sgr A* BLACK HOLE

KEVIN STOVALL, TEVIET CREIGHTON, RICHARD H. PRICE, AND FREDRICK A. JENET

Center for Gravitational Wave Astronomy and Department of Physics and Astronomy, University of Texas at Brownsville, Brownsville, TX 78520, USA
Received 2011 February 25; accepted 2011 September 29; published 2011 December 22

ABSTRACT

According to some models, there may be a significant population of radio pulsars in the Galactic center. In principle, a beam from one of these pulsars could pass close to the supermassive black hole (SMBH) at the center, be deflected, and be detected by Earth telescopes. Such a configuration would be an unprecedented probe of the properties of spacetime in the moderate- to strong-field regime of the SMBH. We present here background on the problem, and approximations for the probability of detection of such beams. We conclude that detection is marginally possible with current telescopes, but that telescopes that will be operating in the near future, with an appropriate multiyear observational program, will have a reasonable chance of detecting a beam deflected by the SMBH.

Key words: black hole physics – Galaxy: nucleus – pulsars: general

Online-only material: color figures

1. INTRODUCTION

Near-infrared observations of stars near our Galaxy’s central supermassive black hole (SMBH) have revealed a larger number of young, massive stars than can be explained by typical star formation models (Ghez et al. 2005; Eisenhauer et al. 2005). This “paradox of youth” (Ghez et al. 2005) has pointed to the development of a possible continuing top-heavy initial mass function (IMF) in the region near the central SMBH (Maness et al. 2007; Nayakshin & Sunyaev 2005). A top-heavy IMF near Sgr A* would imply the existence of a large number of neutron stars in close proximity to the central SMBH. Current estimates suggest that there could be $\gtrsim 10^4$ neutron stars within 1 pc of Sgr A* (Muno et al. 2005), comprising one component of a cusp of massive stellar remnants in the Galactic core (Freitag et al. 2006; Hopman & Alexander 2006). X-ray observations have been consistent with this number of neutron stars (Deegan & Nayakshin 2007) but appear to have ruled out the presence of a larger number of neutron stars (e.g., 40,000). In the innermost regions, the number of pulsars within ~ 0.017 pc of Sgr A* could be as high as ~ 1000 (Pfahl & Loeb 2004), where we take the central SMBH mass to be $4 \times 10^6 M_{\odot}$. For this paper, we will assume the optimistic population density of 1000 pulsars within 0.017 pc of Sgr A*; our results can readily be scaled to more conservative population estimates. We will also follow Pfahl & Loeb in assuming that $n(r)$, the density of pulsars as a function of distance from the Galactic center, falls off as $r^{-3/2}$, so that

$$n = \frac{3}{8\pi} \times 10^6 \text{ pc}^{-3} (r/1 \text{ pc})^{-3/2}. \quad (1)$$

In this paper, we will consider the possibility that an appropriate program to monitor pulsar beams from Sgr A* would detect a beam that is strongly deflected by the central SMBH. Such a system would be of great interest, as precision timing of the radio pulses from such a system would measure the properties of the spacetime through which they propagate. Preliminary work in the case of Schwarzschild black holes, presented in Wang et al. (2009b) and Wang et al. (2009a) (hereafter Paper I and Paper II), has revealed a rich structure and multiplicity of pulses observed in such geometries; subsequent work will look at how pulse timing can be used to measure properties such as the mass and spin of the SMBH, and measure or constrain deviations in the

higher multipoles of the spacetime from the predictions of general relativity. In the present paper we will focus on determining the likelihood of observing a pulsar in such a configuration. To do this we will first calculate the probability that a single pulsar, in orbit around the central SMBH, emits a signal in such a way that it is strongly deflected by the central SMBH, and reaches the Earth. From this we then infer the probability that the signal from one of the assumed number of pulsars is strongly deflected, reaches the Earth, and is detectable by radio telescopes.

The paper continues in Section 2 with a discussion of the model for the pulsar–SMBH system, and with assumptions about pulsar characteristics and telescope sensitivities. The heart of the paper is the method of computation of probabilities in Section 3. Numerical estimates of probability, based on this approach, are given in Section 4, and considerations for an observing program are given in Section 5. In Section 6 we conclude that an observing program, even with current radio telescopes, would have *some* chance of detecting strongly bent pulsar emissions, while later generations of telescopes will significantly increase the likelihood of observing these fascinating systems.

2. BACKGROUND, MODEL, AND ASSUMPTIONS

As a simplification in our probability estimates we take the SMBH in Sgr A* to be a Schwarzschild hole. It is essentially certain, of course, that the SMBH is rotating, but the angular momentum J is currently thought to be less than or of order half of its maximum possible value of GM^2/c , where M is the mass of the SMBH (Melia et al. 2001; Genzel et al. 2003), with some authors finding that observations are consistent with zero spin (Broderick et al. 2011). Typically, the astrophysical properties of Kerr holes differ significantly from those of Schwarzschild holes only when J is very close to GM^2/c . Our preliminary investigations of Kerr holes, in work now underway, confirm this.

While frame dragging by the black hole may slightly increase the probability of detecting beams bent in the prograde sense, and decrease the probability of retrograde-bent beams, these effects largely cancel when considering the population as a whole. Thus the Schwarzschild approximation would appear to

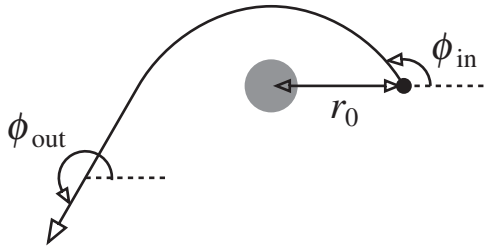


Figure 1. Photon trajectory and the definitions of the angles ϕ_{in} and $\phi_{out} = F(\phi_{in}; r_0)$.

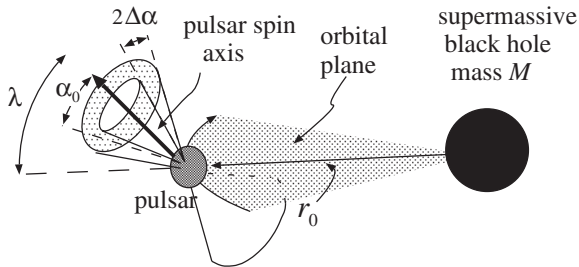


Figure 2. Geometry of the orbit, pulsar spin, and pulsar beam.

be justified for our purposes, in which it is the average properties that are of importance.

We will rely heavily on results in Papers I and II for pulsar beam deflection around a Schwarzschild hole. In those papers ϕ_{in} is the angle between the direction of pulsar emission and the direction radially outward from the central SMBH at the emission event; the angle ϕ_{out} is the angle between that same initial radial direction and the direction in which the pulsar beam is moving when it is asymptotically far from the SMBH, as sketched in Figure 1. In the absence of the bending of the beam, the two angles ϕ_{in} and ϕ_{out} would be equal. The effect of curvature of the beam is encoded in the function F defined by

$$\phi_{out} = F(\phi_{in}; r_0), \quad (2)$$

where r_0 is the distance of the emission point from the SMBH. The computational method for finding the F function is discussed in Papers I and II. A practical approximation for F , useful for the considerations of this paper, is presented in the Appendix.

With the simplification to a nonrotating SMBH, we do not need to consider any angle between the orbit of the pulsar and the spin axis of the SMBH. The geometric parameters of interest are pictured in Figure 2. The inclination of the *pulsar* spin axis with respect to the orbital plane is denoted as λ ; the beam of pulsar emission is taken to have its center at angle α_0 from the spin axis, and to have width angular width $2\Delta\alpha$, so that the pulsar emission is confined between conical surfaces with opening angles $\alpha_0 - \Delta\alpha$ and $\alpha_0 + \Delta\alpha$, as shown in Figure 2.

In Figure 2, r_0 denotes the radial distance of the pulsar from the SMBH at the moment of emission of a beam. We do not assume circular orbits in our probability calculations except in the calculations of orbital times in Section 4.

We will assume that there is no favored alignment of the pulsar spin axis with the pulsar orbital plane, and will take λ to be uniformly distributed over the sky. Within a fraction of a pc from the central SMBH, we expect there to be no significant alignment of the neutron star population with the disk of the Galaxy, so we will take the orientation of the orbital plane also to be randomly distributed over the sphere.

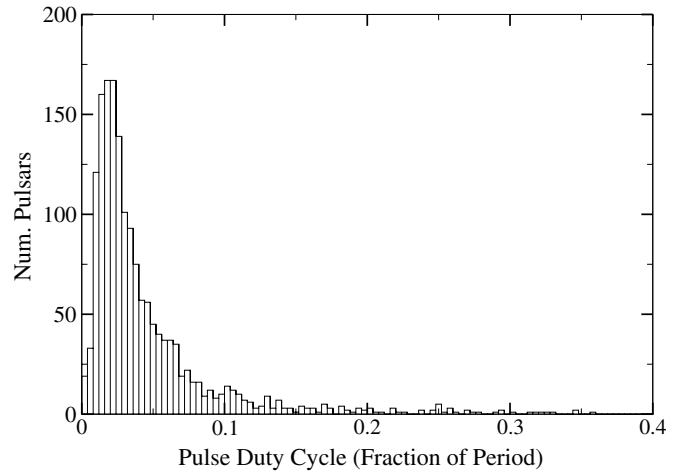


Figure 3. Histogram of the FWHM of currently known pulsars in units of fraction of duty cycle (ATNF Pulsar Catalog 2010).

We will assume the angle α_0 between the pulsar beam and the spin axis to be randomly distributed over the half sphere. Although there is some debate over the alignment of magnetic and spin axes over time (e.g., Weltevrede & Johnston 2008; Young et al. 2010), this is by no means a settled issue, and we therefore make the more generic assumption. We further assume that for every choice of α_0 there is also a beam at $\pi - \alpha_0$. (In our probability estimates, we will avoid double counting in the case when $\alpha_0 + \Delta\alpha > \pi/2$ and the conical regions of the two beams overlap.)

The angular width $\Delta\alpha$ of the pulsar emission is a crucial parameter in the probability of observation of deflected beams. This angular width, seen as the duty cycle in a pulsar reception, depends on the details of the pulsar emission mechanism, which are at best incompletely understood. Observations indicate correlations of beam structure with period, and perhaps with age (Rankin 1996). Here, of necessity, we make do with a simple mean. Figure 3 shows a histogram, for currently known pulsars, of the FWHM of the pulse as a fraction of the pulse duty cycle (Australia Telescope National Facility (ATNF) Pulsar Catalog 2010). The mean of this distribution is 4.6%, so for probability calculations in this paper we will use a duty cycle of 5%, and therefore a value of 9° for $\Delta\alpha$.

Of particular importance is the fact that a strongly bent beam will generally be reduced in intensity in comparison with a directly observed beam; thus our detection probabilities must account for the reduced brightness of the source. In terms of the bending function F of Paper I, the ‘‘amplification’’ factor (generally less than unity) for intensity is given by

$$\frac{I}{I_0} = \frac{\sin \phi_{in}}{\sin(F) (dF/d\phi_{in})}. \quad (3)$$

As a step in understanding how much reduction can be allowed if a pulsar beam is to be observed, we start with the radio luminosity at 1.4 GHz (L band). We will choose our radio luminosities from two separate distributions. The first distribution is from all pulsars for which this quantity has been calculated in the ATNF Pulsar Catalog (2010). In this case, the distribution of pulsar L -band flux densities S , observed at the Earth, would be that shown in Figure 4. Since there are likely to be selection effects present in the distribution of known pulsar luminosities, we will also calculate our probabilities from values chosen from a second distribution described in Faucher-Giguère & Kaspi (2006,

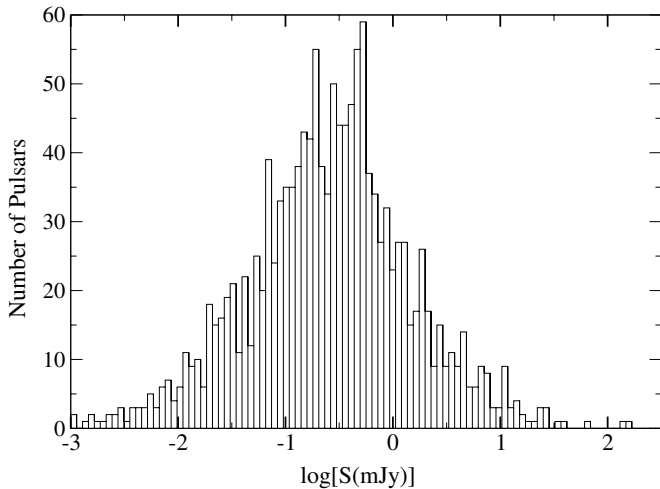


Figure 4. Distribution of pulsar L -band flux density S that would be seen on Earth if all cataloged pulsars were located at the center of the Galaxy (ATNF Pulsar Catalog 2010).

hereafter FGK). This second distribution is a lognormal distribution with $\mu = -1.1$ and $\sigma_{\log L} = 0.9$, which when moved to the Galactic center gives a lognormal distribution with $\mu = -2.9$ while $\sigma_{\log L}$ is unchanged. We present observability results separately for each assumed distribution in Section 4.

While we have used L -band luminosities above, a search for pulsars near the Galactic center will require observations at C band, X band, or Ku band (4–8 GHz, 8–12 GHz, and 12–18 GHz, respectively) to overcome the effects of scattering from plasma in the Galactic cusp. Cordes & Lazio (1997) argue that observations around 10 GHz are optimal, whereas Kramer et al. (2000) contend that the frequency could be pushed as low as 5 GHz. We scale pulsar luminosities to putative search frequencies of 5 GHz, 10 GHz, or 15 GHz assuming a power-law spectrum with spectral index -1.8 (Maron et al. 2000), and give observability results for each case.

The minimum flux detectable at a telescope can be estimated with the following equation in Lorimer & Kramer (2005, hereafter LK), originally from Dewey et al. (1985):

$$S_{\min} = \frac{(\text{SNR}_{\min})\beta_0 S_{\text{sys}}}{\sqrt{n_p t_{\text{obs}} \Delta f}} \sqrt{\frac{W}{P - W}}. \quad (4)$$

Here W and P are, respectively, the pulsar pulse width and period. From our assumption that W/P is 5% we get $\sqrt{W/(P - W)} = 0.23$. The parameter β_0 is a correction factor for imperfections in data collection. Most current pulsar detection systems are multibit systems with β_0 close to 1, and this is the value we shall use. For n_p , the number of polarizations recorded and summed in the detection process, we will use $n_p = 2$ because typically two polarizations are summed during pulsar detection scans. SNR_{\min} is the minimum detectable signal-to-noise ratio required in a search; we will take this to be 8.

For the time pointed at the source, t_{obs} , we will assume a 1 hr observing time. The bandwidth of the recorded data Δf depends highly on the pulsar detection instruments used at a particular telescope. Bandwidths at the frequencies in which we are interested typically range from 500 MHz to 3 GHz. S_{sys} is the system equivalent flux density, which depends strongly on the collecting area of the telescope and the raw antenna sensitivity (see LK). Table 1 details the relevant characteristics

Table 1
Theoretical S_{\min} Values for Two Existing Radio Telescopes (Parkes, GBT) and One Planned Radio Telescope (SKA) at Three Frequency Bands

Telescope	Frequency Band	S_{sys} (Jy)	Δf (MHz)	S_{\min} (mJy)
Parkes	C band	43	500	.042
	X band	46	500	.045
	Ku band	120	500	.14
GBT	C band	8	2000	.0039
	X band	15	2400	.0066
	Ku band	18	3500	.0066
SKA	C band	.23	2000	.00007
	X band	.23	2400	.00006
	Ku band	.23	3500	.00005

Notes. The S_{sys} values for the existing radio telescopes are measured system equivalent flux densities and the Δf values are for current receivers. The S_{sys} values for the SKA are theoretical values and the Δf values were chosen to be the same as the GBT receivers.

of the current Parkes telescope in Australia and Green Bank Telescope (GBT) in the USA, as well as the planned Square Kilometre Array (SKA).

3. PROBABILITY CALCULATIONS

In this section, we show how to calculate the probability that radiation from a single pulsar is detectable by a telescope on Earth, after having passed through the strong-field region of the black hole. This calculation naturally breaks down into two parts: determining what orientations of the pulsar and black hole produce strongly bent beams, and determining where the Earth must be positioned relative to the system in order to detect those beams.

In Paper II, it was shown that for any relative position of pulsar, black hole, and Earth, there are a set of directions, called “keyholes,” in which a photon could be emitted from the pulsar, pass around the black hole, and arrive at the Earth. These keyholes are typically within a few Schwarzschild radii of the black hole, so when the pulsar is far (many Schwarzschild radii) from the black hole, we can treat the keyhole as co-located with the black hole: that is, the pulsar beam must sweep across the black hole. The first part of the probability calculation is to determine for what fraction of the pulsar’s orbit it is in a position to illuminate the black hole with its beam.

We view the system from the perspective of the pulsar, so that the black hole traverses the sky of the pulsar along a great circle corresponding to the orbital plane. (This great circle in the pulsar sky does not imply that the pulsar–SMBH distance is constant.) Meanwhile, the pulsar spins about its rotation axis, and emits radiation in a cone offset from that axis: once per pulsar rotation the cone sweeps out an annulus in the sky of the pulsar. This is illustrated in Figure 5, where α_0 , $\Delta\alpha$, and λ have the meaning described in Section 2 and pictured in Figure 2.

With Figure 5(b) we introduce the angle β , the total arc length (if any) over which the annulus intersects the orbital plane. When calculating β , it is useful to focus on one hemisphere at a time and to label the two edges of the pulsar’s radiation cone. We will define these two edges as $\alpha_1 = \alpha_0 - \Delta\alpha$ and $\alpha_2 = \alpha_0 + \Delta\alpha$. We break the calculation of β into three cases, with one case having two subcases. The first case is that in which the orbital plane of the system is never illuminated by the pulsar’s radiation, $\alpha_2 < \lambda$, as shown in Figure 6. In this

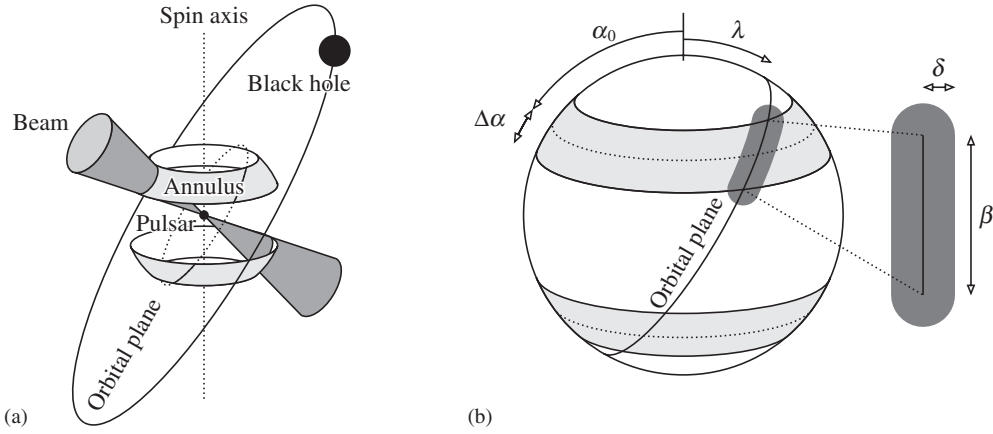


Figure 5. Geometry of a pulsar–black-hole system as seen from the pulsar’s reference frame. Panel (a) shows how the pulsar beam sweeps out an annular region in the pulsar’s sky, which may intersect with the orbital plane of the pulsar–black-hole system. Panel (b) shows the pulsar sky and labels the angles describing the orientation: λ is the angle between the spin axis and orbital plane, α_0 is the angle between the spin axis and the center of the illuminated annulus (or beam), and $\Delta\alpha$ is the half-width of the annulus (or beam). The zoom on the right shows the region in the pulsar’s sky in which the Earth can lie if the photons reaching the Earth from the strong-field regime are to be bent by no more than an angle δ .

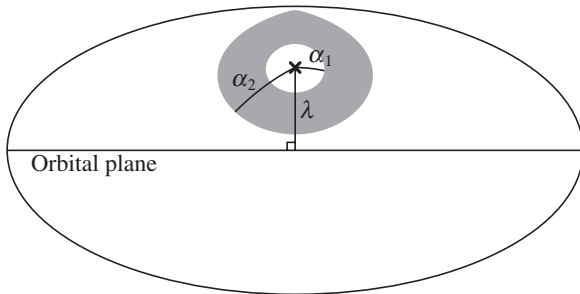


Figure 6. Schematic of the pulsar sky for case 1, in which the orbital plane does not intersect the annulus.

case, the value of β is trivially zero. The second case is the case in which the orbital plane passes between the outer and inner edges of the annulus: $\alpha_1 \leq \lambda < \alpha_2$. This case has two subcases. In the first subcase, that for $\alpha_2 > \pi/2$, the entire orbital plane is illuminated by the pulsar, as shown in Figure 7(a). The value of β in this case is the entire range π that lies in that hemisphere of the pulsar’s sky. (Remember that we are assuming symmetric emission about the pulsar’s rotational plane, so that the two beams together illuminate the full 2π range of the orbital plane.) The second subcase, when $\alpha_2 \leq \pi/2$, has the outer edge of the annulus intersecting the orbital plane twice, as shown in Figure 7(b). In this case, β can be found from the spherical triangle version of Pythagoras’s theorem, applied to the triangle with hypotenuse α_2 and sides λ and $\beta/2$: $\cos \alpha_2 = \cos \lambda \cos \beta/2$, whence $\beta = 2 \arccos(\cos \alpha_2 / \cos \lambda)$. The final case has both the outer and inner edges of the annulus crossing the orbital plane, $\alpha_1 > \lambda$, as illustrated in Figure 8. The

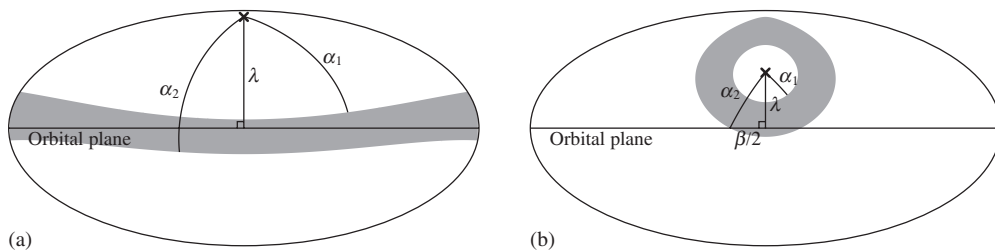


Figure 7. Schematic of pulsar sky for case 2, in which the orbital plane passes between the outer and inner edges of the annulus. In panel (a), the orbital plane is entirely contained within the annulus. In panel (b), it crosses the outer edge of the annulus at two points symmetric about the meridian containing the spin axis.

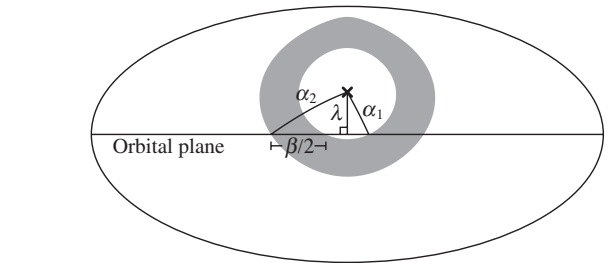


Figure 8. Schematic of pulsar sky for case 3, in which the orbital plane intersects both the inner and outer edges of the annulus.

calculation proceeds as in the previous case, but considers only the range of β between the triangles with hypotenuses α_2 and α_1 : $\beta = 2 \arccos(\cos \alpha_2 / \cos \lambda) - 2 \arccos(\cos \alpha_1 / \cos \lambda)$. The cases and calculations for β are summarized in Table 2.

The second part of the probability calculation is to determine how often the Earth will be in a position to detect strongly bent beams from the system. This imposes geometric limitations to ensure that we are considering beams that are significantly deflected by the black hole, but that are not deflected so strongly that they are attenuated to a flux too low to be detected. These constraints turn out to place limits on the acceptable range of ϕ_{out} .

The determination of this range is shown in Figure 9 for the case $r_0 = 100M$. This figure shows the dramatic amplification at $\phi_{\text{out}} = \pi$, corresponding to strong lensing. For ϕ_{out} slightly less than π , the attenuation factor is unity, and the bending is not significant. There is bending for $\phi_{\text{out}} < \pi$, but the range of ϕ_{out} for which there is significant bending is small. Moreover,

Table 2
Formulae for the Overlap Angle β of the Pulsar Beam with the Orbital Plane

Case	Condition	β Calculation
1	$\alpha_2 \leq \lambda$	$\beta = 0$
2a	$\alpha_1 \leq \lambda < \alpha_2$	$\left\{ \begin{array}{l} \alpha_2 \geq \pi/2 \\ \alpha_2 < \pi/2 \end{array} \right.$
2b		$\beta = \pi$ $\beta = 2 \arccos\left(\frac{\cos \alpha_2}{\cos \lambda}\right)$
3	$\lambda < \alpha_1$	$\beta = 2 \arccos\left(\frac{\cos \alpha_2}{\cos \lambda}\right) - 2 \arccos\left(\frac{\cos \alpha_1}{\cos \lambda}\right)$

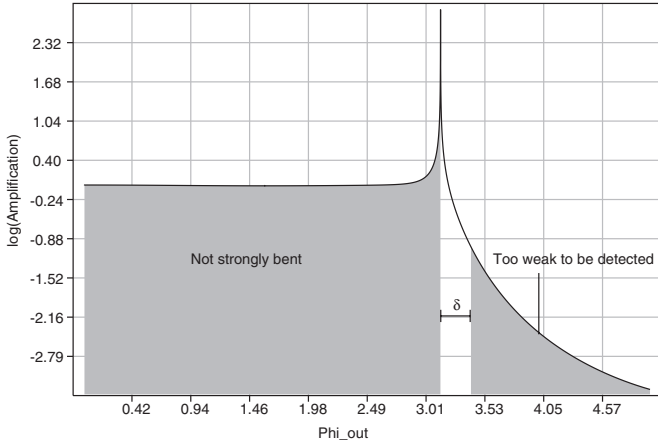


Figure 9. Intensity ratio I/I_0 as a function of ϕ_{out} , for $r_0 = 100 M$. The shaded regions show the ranges of ϕ_{out} that are not of interest either because the pulsar beam is too weakly deflected or because it is too strongly attenuated.

this range is even smaller than in Figure 9 for the larger, more relevant values of r_0/M . As a convenient approximation, therefore, we will consider “strong bending” only for $\phi_{\text{out}} \geq \pi$. The figure shows that as ϕ_{out} increases beyond π the attenuation becomes greater and greater.

Our approach will be to specify a radius of emission r_0 and a minimum acceptable value of I/I_0 . From a calculation like that shown in Figure 9 we then find the value of the angle δ , the value of $\phi_{\text{out}} - \pi$ at which the attenuation is that of the minimum acceptable value of I/I_0 . This value of δ determines the range of directions in which the Earth must be located if an Earth telescope is to detect the beam: the Earth must lie no more than an angle δ from the pulsar–black-hole axis.

The corresponding region on the pulsar sky is illustrated in Figure 5(b). Since δ is typically very small, we can express this area using a flat-space approximation: $2\beta\delta + \pi\delta^2$. The probability that observers on Earth can detect strongly bent beams from a given pulsar is given by the size of this area over the angular area of one hemisphere (again, we assume symmetry across the rotation plane of the pulsar):

$$P_1 = \frac{2\beta\delta + \pi\delta^2}{2\pi}. \quad (5)$$

This of course assumes nonzero β : if $\beta = 0$, the black hole is not illuminated by the pulsar, and there are no strongly bent beams, so $P_1 = 0$. Note that β is a function of the underlying parameters λ , α_0 , and $\Delta\alpha$, and δ is a function of the underlying parameters r_0/M and I_{min}/I_0 .

4. RESULTS

Now that we have shown how to calculate the probability of Earth-based detection of a particular pulsar, we will describe how we estimated the number of pulsars that would be detected

Table 3

Minimum Detectable Fluxes S_{min} and Number of Detectable Pulsars $P_{\text{tot}}^{\text{ATNF}}$, $P_{\text{tot}}^{\text{FGK}}$ (assuming intrinsic luminosity distributions from ATNF and FGK, respectively) for Two Existing Radio Telescopes (Parkes, GBT) and One Planned Radio Telescope (SKA)

Telescope Name	Frequency Band	S_{min} (mJy)	$P_{\text{tot}}^{\text{ATNF}}$	$P_{\text{tot}}^{\text{FGK}}$
Parkes	C band	.042	8.21	.189
	X band	.045	3.53	.0490
	Ku band	.14	.839	.00548
GBT	C band	.0039	27.0	1.45
	X band	.0066	11.5	.331
	Ku band	.0066	7.61	.167
SKA	C band	.00007	113	16.6
	X band	.00006	79.1	9.58
	Ku band	.00005	65.7	7.05

given assumptions about the distributions of pulsar characteristics. We ran Monte Carlo simulations that selected λ from a uniform distribution of $\cos \lambda$, so that the direction of the pulsar spin axis was uniformly distributed over the sky; similarly, α_0 was chosen from a uniform distribution of $\cos \alpha_0$. Then a value for the pulsar’s flux, S , was chosen from the distribution shown in Figure 4. Lastly, a value of r_0/M was chosen from the distribution in Equation (1); we cut this distribution off at $r_0/M = 400,000$ since pulsars beyond that point contribute little to the total probability (see below).

The simulations took the pulsar parameters (r_0 , S) chosen by the Monte Carlo method. From these a determination of the minimum value of I/I_0 was made (equivalently S_{min}/S) that can be detected for those pulsar parameters. From I/I_0 and r_0 , the value of δ was determined. The value of β was determined through the calculations described in the previous section applied to the values of λ and α_0 chosen by the Monte Carlo method. The justification for using $\Delta\alpha = 9^\circ$ has been explained in Section 2. P_1 was then calculated with Equation (5). This gives us the probability that a single pulsar’s beam will explore the black hole’s strong gravitational field and still be detectable once it reaches the Earth. Monte Carlo simulations were repeated to ensure that results were consistent to better than 1%. We then multiplied our result by the total number of pulsars out to $r_0 = 400,000$, according to the Pfahl and Loeb distribution of Equation (1). The result is the total number of pulsars (P_{tot}) that will, at some point in their orbit about the central SMBH, both illuminate the strong gravitational field and be detectable at Earth. Table 3 gives this number for the three telescopes considered in Section 2, in three different frequency bands, for the two luminosity distributions ATNF and FGK.

The number of pulsars that are observable at some point in their orbit is not directly relevant if the orbital time is much larger than the duration of an observing program. For this reason we introduce a more useful number, the “observability,” P_{obs} , to describe the expected number of pulsars detectable in a limited-time observing program. In order to calculate this

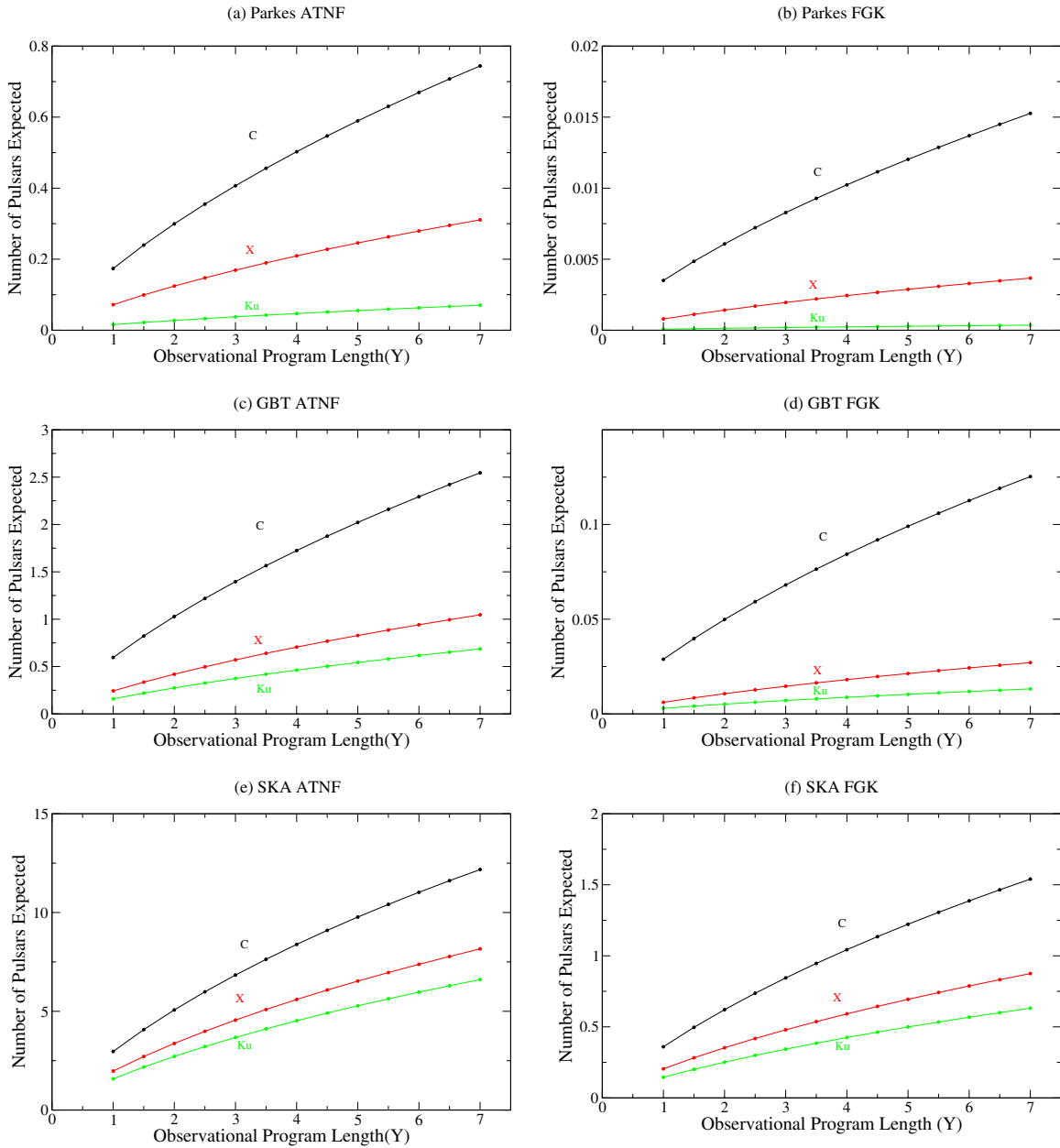


Figure 10. Expected number of pulsars observed having strongly bent beams as a function of observational program duration for three different telescopes (Parkes, GBT, SKA) and two luminosity distributions (ATNF, FGK). Curves are labeled with the observing frequency band.

(A color version of this figure is available in the online journal.)

number, we ran the Monte Carlo simulations with a specified observational program duration (L). Once P_1 was calculated, we then compared the pulsar’s orbital period (T) to L . If T was less than or equal to L , then P_{obs} was taken to be P_1 . If T was greater than L , then P_1 was replaced by

$$P_{\text{obs}} = \frac{P_1 \times L}{T}, \quad (6)$$

and the result was multiplied by the total number of pulsars. Figure 10 shows the results of the Monte Carlo simulations for observational program durations ranging from one year to seven years.

Figure 11 shows the variation in the number of pulsars detected, for $S_{\text{min}} = 0.0066$ mJy at 5 GHz, as the cutoff radius is changed, and justifies our use of the cutoff at $r_0/M = 4 \times 10^5$.

Other values of S_{min} and observing frequency give similar results.

5. OBSERVING PROGRAMS AND STRATEGIES

A natural first question about observing strongly deflected beams is “how will we know that they are strongly deflected?” The answer starts with the fact that the angle through which the beam is “strongly” deflected is not large. For our paradigmatic case, $r_0 = 10^4 M$, the bending is approximately 0.036 rad. For larger r_0 the deflection, for a given S_{min} , is even smaller.

Since the “strong” deflection is small, we will receive a deflected beam only when the emitting pulsar, the SMBH, and the Earth are almost on a straight line. Since pulsar beam widths are large compared to the deflection, this means that if the Earth receives the deflected beam, it will also receive the direct beam. The geometry of the direct and deflected beams is shown in

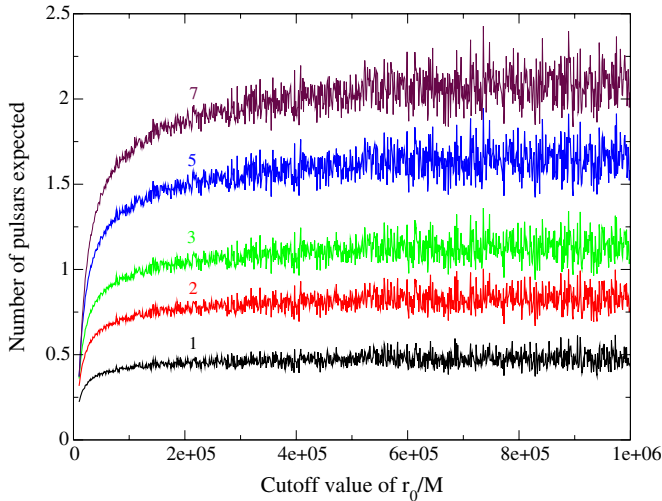


Figure 11. Number of pulsars expected, for $S_{\min} = 0.0066$ mJy, at 5 GHz as a function of the cutoff r_0/M for the distribution in Equation (1) and the ATNF luminosity distribution. Each curve is labeled with the number of years assumed for the search.

(A color version of this figure is available in the online journal.)

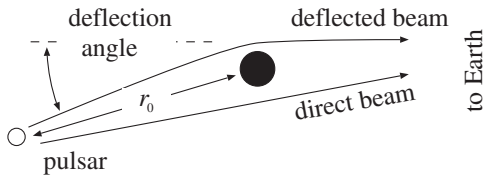


Figure 12. Geometry of the observation of direct and deflected beams.

Figure 12, where we see that the angle, at reception, of the direct and deflected beams is not of order r_0 divided by the Earth–SMBH distance (8 kpc), but rather is of order of that number multiplied by the deflection angle. The result, an angle of order 10^{-8} rad, is less than the resolution of radio telescopes. We conclude that any monitoring of the innermost region of Sgr A* for a deflected beam will also monitor for a direct beam.

The criterion for the detection of a strongly deflected beam will be that it is one of a pair of pulses detected with very similar pulse periods, differing only due to a phase modulation caused by variations in the propagation times along the two paths: the two sets of pulses will differ in pulse period by a fractional amount of order the pulsar velocity divided by c . (See Papers I and II for more detail on phase effects and intensity effects of deflection.) If a deflected beam is detected we therefore assume that it will be relatively simple to identify it as deflected.

If the Pfahl and Loeb distribution of Equation (1) is approximately valid with a pulsar luminosity distribution similar to known (ATNF) pulsars, the results of the previous section, especially Figure 10, suggest that there is a reasonable chance of observing one or more strongly deflected pulsar beams with an observing program of 3–5 years using existing telescopes, particularly if Kramer et al. (2000) are correct and the search can be carried out at 5 GHz. More pessimistically, if we assume luminosity selection effects from FGK, the chances of detecting such beams with existing telescopes are slim, and we must await more sensitive instruments such as the SKA.

An appropriate multiyear observing program can be carried out “in background” at a telescope. Observations must be made sufficiently frequently not to miss the relatively short epoch during which the pulsar/SMBH/Earth alignment leads to a strongly deflected beam meeting the I/I_0 criterion. This epoch

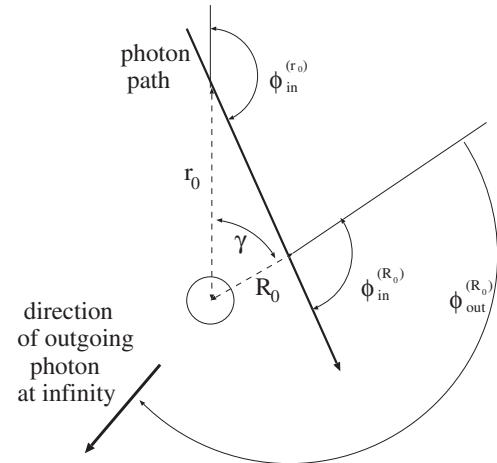


Figure 13. Flat spacetime propagation from large radius to very large radius. Angles ϕ_{in} for the large and the very large emission radius are distinguished with the superscripts (R_0) and (r_0), respectively.

is of order of the orbital time multiplied by the ratio $\delta/(2\pi)$. For our prototypical choice $r_0 = 10^4 M$, this epoch is on the order of a week. Searches for deflected beams in Sgr A*, therefore, would have to be made every other day. The observing session would be of a duration of that used for any other pulsar search, on the order of 1 hr. Longer observations might be considered, in view of the effect shown in Equation (4) of t_{obs} on S_{\min} and hence on the I/I_0 cutoff.

An important question to ask is why we do not yet have evidence of the assumed large population of pulsars in Sgr A*. Surveys of the Galactic center at 3.1 GHz and 8.4 GHz with the Parkes observatory (Johnston et al. 2006), and at 2 GHz with the GBT (Deneva et al. 2009), discovered a total of five highly dispersed pulsars, but none within $10'$ of Sgr A*. It is quite possible, however, that these surveys are limited by scattering at low frequencies due to plasma at the Galactic center, and by reduced sensitivity at higher frequencies due to the negative spectral index of pulsar emissions. Overcoming these effects might require observations at frequencies of 5 GHz (Kramer et al. 2000) or 10 GHz (Cordes & Lazio 1997), using the most sensitive telescopes and receivers available at those frequencies.

It should be noted that, at least to some extent, monitoring the Galactic center for strongly deflected beams would constitute a more general search for pulsars in that region. The possibility of detecting deflected beams and making measurements of the parameters of the SMBH provides added scientific motivation for such a survey.

6. CONCLUSIONS

Our estimates suggest that a multiyear program that monitors Sgr A* with radio observations for 1 hr every other day has a very small but non-negligible probability of detecting pulsar beams that have been strongly deflected by our Galaxy’s SMBH. With instruments coming in the near future, in particular the SKA, the probability should become high enough so that a three-year observational program might optimistically detect such beams from multiple pulsars, or, in the absence of detections, would constrain the more optimistic models for the pulsar population in the Galactic cusp.

Our estimates in this paper constitute a first step in the study of probabilities of detection of a strongly deflected beam. The intention was to establish whether the probabilities are so small that observations are out of the question, or so large that

current observations rule out models, like that of Pfahl & Loeb (2004), with a significant density of pulsars in Sgr A*. The estimates in this paper establish neither extreme: a concerted observing program with the best current telescopes would not be guaranteed to make a detection, but under optimistic models or with improved instruments could plausibly detect strongly bent beams from a (small) number of pulsars. This provides motivation for such a program and also for further study of the problem of pulsar beam deflection by SMBHs.

Such an improved study would have to include effects of spin of the SMBH, and of eccentricity of orbits. While our approach of using averages and simple assumptions was appropriate for the purpose of this paper, effects due to SMBH spin, and high eccentricity, could increase the parameter space of pulsar configurations whose beams can reach the Earth. Such work is now underway.

The most exciting result of these preliminary estimates is their indication that we are potentially on the verge of detecting a new phenomenon: pulsar beams that have passed through the strong-field region of the SMBH at the center of our Galaxy, beams that can bring us information about the properties of the SMBH and its surrounding spacetime might be inaccessible in any other way.

We gratefully acknowledge support by the National Science Foundation under grants AST0545837, PHY0554367, and HRD0734800. We thank the Center for Gravitational Wave Astronomy at the University of Texas at Brownsville. We also thank an anonymous referee for many helpful suggestions.

APPENDIX

We are primarily interested in values of ϕ_{in} that are only slightly smaller than π . In this case the photon path starting at some very large radius will penetrate to small radii, and almost all the bending will take place at small radii. We can then find the bending for emission from the very large radius, say $r_0 = 10,000 M$, by considering the bending only interior to a smaller large radius, say $R_0 = 100 M$. In effect, we are considering the large radius region from R_0 to r_0 to be flat space, as illustrated in Figure 13. From the curve $F(\phi_{\text{in}}; r)$ for $R_0 = 100 M$, therefore, we can infer the curve for $r_0 = 10,000 M$, and for all larger radii (provided, of course, that ϕ_{in} is near π so that both R_0 and r_0 are much larger than the radii at which the bending occurs).

To find $\phi_{\text{out}}^{(r_0)}$ for a photon emitted at a very large r_0 , we choose the smaller R_0 along the future path of the photon to be a radius for which we know the curve $\phi_{\text{out}}^{(R_0)} = F(\phi_{\text{in}}^{(R_0)}; R_0)$. Here superscripts (r_0) and (R_0) distinguish the angles associated with the two radii. The Euclidean geometry relating $\phi_{\text{in}}^{(r_0)}$ and $\phi_{\text{in}}^{(R_0)}$ is given by the law of sines to be

$$\phi_{\text{in}}^{(R_0)} = \sin^{-1} \left(\frac{r_0}{R_0} \sin \phi_{\text{in}}^{(r_0)} \right), \quad (\text{A1})$$

and we choose the branch of \sin^{-1} so that $\phi_{\text{in}}^{(R_0)} > \pi/2$.

We next note that ϕ_{out} for the photon starting at R_0 is less than ϕ_{out} for that same photon world line considered to start at r_0 , in flat space, according to

$$\phi_{\text{out}}^{(r_0)} = \phi_{\text{out}}^{(R_0)} + \gamma. \quad (\text{A2})$$

With γ evaluated in terms of the ingoing angles, this becomes

$$\phi_{\text{out}}^{(r_0)} = \phi_{\text{out}}^{(R_0)} + \phi_{\text{in}}^{(r_0)} - \phi_{\text{in}}^{(R_0)}. \quad (\text{A3})$$

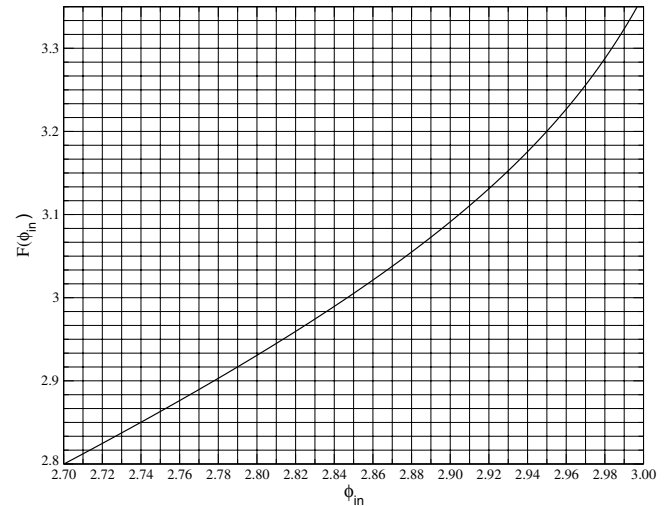


Figure 14. Bending function $\phi_{\text{out}} = F(\phi_{\text{in}})$ for bending angles near π , for an initial radius $R_0 = 100 M$.

From a combination of Equations (A1) and (A3), written in terms of the function $F(\phi; r)$, the full expression can be given as

$$F(\phi; r_0) = \phi + F \left[\sin^{-1} \left(\frac{r_0}{R_0} \sin \phi \right); R_0 \right] - \sin^{-1} \left(\frac{r_0}{R_0} \sin \phi \right). \quad (\text{A4})$$

Thus, knowing the F function for any (sufficiently large) R_0 , we can evaluate it for any larger r_0 , and thus determine the maximum deflection angle δ via Equation (3). Figure 14 shows our reference bending function for a radius $R_0 = 100 M$.

REFERENCES

- ATNF Pulsar Catalog 2010, <http://www.atnf.csiro.au/research/pulsar/psrcat>
- Broderick, A. E., Fish, V. L., Doeleman, S. S., & Loeb, A. 2011, *ApJ*, **735**, 110
- Cordes, J. M., & Lazio, T. J. W. 1997, *ApJ*, **475**, 557
- Deegan, P., & Nayakshin, S. 2007, *MNRAS*, **377**, 897
- Deneva, J. S., Cordes, J. M., & Lazio, T. J. W. 2009, *ApJ*, **702**, L177
- Dewey, R. J., Taylor, J. H., Weisberg, J. M., & Stokes, G. H. 1985, *ApJ*, **294**, L25
- Eisenhauer, F., Genzel, R., Alexander, T., et al. 2005, *ApJ*, **628**, 246
- Faucher-Giguère, C.-A., & Kaspi, V. M. 2006, *ApJ*, **643**, 332 (FGK)
- Freitag, M., Amaro-Seoane, P., & Kalogera, V. 2006, *J. Phys. Conf. Ser.*, **54**, 252
- Genzel, R., Schödel, R., Ott, T., et al. 2003, *Nature*, **425**, 934
- Ghez, A. M., Salim, S., Hornstein, S. D., et al. 2005, *ApJ*, **620**, 744
- Hopman, C., & Alexander, T. 2006, *J. Phys. Conf. Ser.*, **54**, 321
- Johnston, S., Kramer, M., Lorimer, D. R., et al. 2006, *MNRAS*, **373**, L6
- Kramer, M., Klein, B., Lorimer, D., et al. 2000, in *ASP Conf. Ser. 202, IAU Colloq. 177: Pulsar Astronomy—2000 and Beyond*, ed. M. Kramer, N. Wex, & R. Wielebinski (San Francisco, CA: ASP), 37
- Lorimer, D. R., & Kramer, M. 2005, *Handbook of Pulsar Astronomy* (Cambridge: Cambridge Univ. Press) (LK)
- Maness, H., Martins, F., Trippe, S., et al. 2007, *ApJ*, **669**, 1024
- Maron, O., Kijak, J., Kramer, M., & Wielebinski, R. 2000, *A&AS*, **147**, 195
- Melia, F., Bromley, B. C., Liu, S., & Walker, C. K. 2001, *ApJ*, **554**, L37
- Muno, M. P., Pfahl, E., Baganoff, F. K., et al. 2005, *ApJ*, **622**, L113
- Nayakshin, S., & Sunyaev, R. 2005, *MNRAS*, **364**, L23
- Pfahl, E., & Loeb, A. 2004, *ApJ*, **615**, 233
- Rankin, J. M. 1996, in *ASP Conf. Ser. 105, IAU Colloq. 160: Pulsars: Problems and Progress*, ed. S. Johnston, M. A. Walker, & M. Bailes (San Francisco, CA: ASP), 237
- Wang, Y., Creighton, T., Price, R. H., & Jenet, F. A. 2009a, *ApJ*, **705**, 1252 (Paper II)
- Wang, Y., Jenet, F. A., Creighton, T., & Price, R. H. 2009b, *ApJ*, **697**, 237 (Paper I)
- Weltevrede, P., & Johnston, S. 2008, *MNRAS*, **387**, 1755
- Young, M. D. T., Chan, L. S., Burman, R. R., & Blair, D. G. 2010, *MNRAS*, **402**, 1317